Structure and stability of graphene nanoribbons in oxygen, carbon dioxide, water, and ammonia

Ari P. Seitsonen

IMPMC, Université Paris 6 et 7, CNRS, IPGP, 140 rue de Lourmel, F-75015 Paris, France
and Physikalisch-Chemisches Institut, Universität Zürich, Winterthurerstrasse 190, CH-8057 Zürich, Switzerland

A. Marco Saitta, Tobias Wassmann, Michele Lazzeri, and Francesco Mauri

IMPMC, Université Paris 6 et 7, CNRS, IPGP, 140 rue de Lourmel, F-75015 Paris, France

We determine, by means of density-functional theory, the stability and the structure of graphene-nanoribbon (GNR) edges in presence of molecules such as oxygen, water, ammonia, and carbon dioxide. As in the case of hydrogen-terminated nanoribbons, we find that the most stable armchair and zigzag configurations are characterized by a nonmetallic/nonmagnetic nature, and are compatible with Clar's sextet rules, well known in organic chemistry. In particular, we predict that, at thermodynamic equilibrium, neutral GNRs in oxygen-rich atmosphere should preferentially be along the armchair direction while water-saturated GNRs should present zigzag edges. Our results promise to be particularly useful to GNRs synthesis since the most recent and advanced experimental routes are most effective in water and/or ammonia-containing solutions.

PACS number(s): 71.15.Mb, 71.20.Tx, 73.20.At, 73.22.Pr

I. INTRODUCTION

Narrow graphene nanoribbons (GNRs) (Ref. 1) are carbon allotropes that promise to combine the high carrier mobility of graphene[2] with a semiconducting nature due to quantum confinement in the lateral direction. The resulting systems are likely to be suitable for direct application as channel in field-effect transistors and other semiconducting devices. The design of GNRs, and more generally of graphene samples with controlled edges, is crucial in determining their electronic and transport properties. Among the variety of reported experimental approaches, three routes, intensely explored in the last couple of years, seem at the frontier of current research: (i) lithographic patterning;[3–6] (ii) sonochemical methods;[7,8] (iii) metallic nanoparticle chemical etching (unzipping) of graphite/graphene (nanotubes).[9–14] Gaining control of the edge profiles and structures is of course one of the most important issues to solve, somehow defining the potential impact of these approaches. The observation of graphene edges[15,16] and/or GNR (Refs. 7 and 14) profiles at atomic-scale resolution indicates that the mentioned experimental methods are capable of producing smooth, likely nonchiral (i.e., no mixing of zigzag and armchair direction), edges. However, little is known on *how* to achieve either zigzag or armchair edges and about the actual chemical termination of the unsaturated carbon bonds.

In this regard, the huge number of theoretical works that recently appeared in the literature on GNRs (Refs. 17–27) has almost exclusively focused on single-hydrogen saturation of the edge carbon atoms. This was mainly due to the surprising discovery of spin-polarized electronic states localized on the edges of zigzag GNRs,[17,18] possibly turning them into half metals under high electric fields,[19,20] and spurring great interest in view of possible applications in future spintronics. However, we have recently[28,29] pointed out that the single-H-terminated zigzag GNRs, and thus all those fascinating electronic and magnetic properties they exhibit, might only be stable at very difficult experimental conditions.

The hydrogen case study is presently extended to GNRs terminated with other relevant atoms and molecules.[30–35] In fact, as mentioned above, experiments are often performed in aqueous or ammonia-containing solutions or in oxidizing conditions. More generally water and oxygen contamination (for example, in air) is extremely important in determining the electronic properties of graphitic systems. For example, the chemical reactions that induce the unzipping of carbon nanotubes are thought to leave O-terminated zigzag GNRs as end products.[11] In this work we thus report density-functional theory (DFT) calculations of the energetics and structures of various GNR edges terminated with atmospheric molecules, such as oxygen, water, and ammonia, as functions of the respective chemical potentials. The work is organized as follows: in Sec. II we describe the theoretical method and define the relevant thermodynamic quantities; in Sec. III we present our systematic study on oxygen-terminated zigzag and armchair GNRs. In Sec. IV we report our results on selected GNRs in presence of water and ammonia molecules; discussion on the electronic and magnetic properties and comparisons with experimental data are drawn in Sec. V while Sec. VI is devoted to conclusions and perspectives.

II. METHOD

DFT calculations were performed with the PWSCF code of the QUANTUM ESPRESSO suite[36] in a plane-wave/ultrasoft-pseudopotential approach, adopting the generalized gradient approximation (GGA) from Ref. 37 for the exchange-correlation functional. We used a kinetic-energy/charge cutoff of 30/300 Ry. Edges were simulated within a supercell geometry using a vacuum layer of 9.5 Å between two edges and of 10.6 Å between two graphene planes. L was fixed according to the lattice constant of graphene (2.46 Å) and atomic positions were allowed to fully relax. In the case of armchair edges, the width of the ribbons was about 22.4 Å and for zigzag ribbons about 28.9 Å. Electronic integrations were done using equidistant, consistent grids along the periodic direction of the ribbon corresponding to 12 k points in the smallest unit cell. Denser grids have been occasionally used in the presence of metallic/magnetic states. We limited
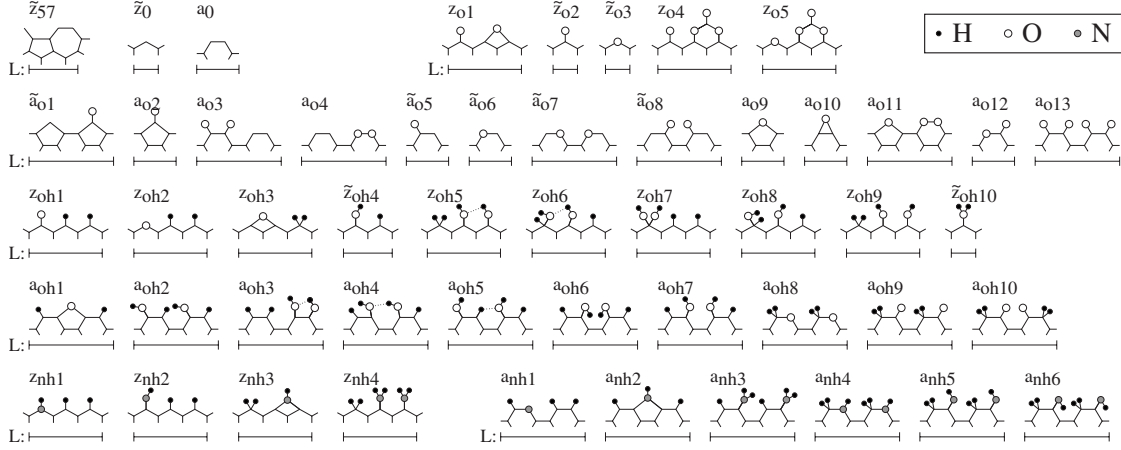
FIG. 1. Scheme and labeling of the oxygen- (right top line and second line from top), water- (third and fourth lines from top), and ammonia-terminated (bottom line) edges of a graphene nanoribbon considered in this work. Hydrogen, oxygen, and nitrogen atoms are the small circles while carbon atoms are not explicitly represented; dashed lines indicate hydrogen bonds. The structures are periodic along the ribbon edge with periodicity L and are ordered with respect to increasing O and N density and, at equal density, to increasing formation energy. A tilde over an edge label indicates that structure is not an aromatic one.

our study to the thermodynamic stability of neutral systems, and as such kinetics and charge effects are not included. In fact, although graphene edges and GNR can be obtained experimentally in charged atmospheres, their technological interest resides in their electronic properties in the neutral state, i.e., at a Fermi level as close as possible to the Dirac point of the graphene band structure. We argue that GNRs and graphene edges obtained at high doping level might be extremely reactive when brought back to neutrality and recombine to form more stable edge structures.

III. OXYGEN AND CARBON DIOXIDE

As in Ref. 28, we calculate the zero-temperature edge-formation energy per unit length as follows:

$$\mathcal{E}_{O_2} = \frac{1}{2L}\left(E^{ribb} - N_C E^{blk} - \frac{N_O}{2} E_{O_2} \right), \qquad (1)$$

where E^{ribb}, E^{blk}, and E_{O_2} are the total energy of the ribbon supercell, of one atom in "bulk" graphene, and of the isolated O_2 molecule. N_C (N_O) are the number of carbon (oxygen) atoms in the supercell while L the length of the unit cell (see Fig. 1). $\mathcal{E}_{O_2}$ can be used to determine the stability of different structures as a function of the experimental conditions.[38] In presence of molecular O_2 gas, at a given chemical potential μ_{O_2}, the relative stability is obtained by comparing $G_{O_2} = \mathcal{E}_{O_2} - \rho_O \mu_{O_2}/2$, where $\rho_O = N_O/(2L)$. At the absolute temperature T and for a partial O_2 pressure P,[39]

$$\mu_{O_2} = H°(T) - H°(0) - TS°(T) + k_B T \ln\left(\frac{P}{P°}\right), \qquad (2)$$

where $H°$ ($S°$) is the enthalpy (entropy) at the pressure $P°$ = 1 bar obtained from Ref. 40. In presence of monatomic-oxygen gas one should use $G_O = \mathcal{E}_O - \rho_O \mu_O$, where $\mathcal{E}_O = \mathcal{E}_{O_2} - \rho_O \times 2.86$ eV, i.e., the binding energy *per atom* of the O_2 molecule in DFT-GGA. The most stable structures are then

obtained, as in Ref. 28, by comparing their respective Gibbs free energy G_{O_2} as function of the (molecular) oxygen chemical potential. G is linear in μ, the slope being determined by ρ_O. For a given value of μ the most stable structure is the one with the lowest value of G, thus, by increasing μ (i.e., going to an environment richer in oxygen) the favorable structures will be those with higher oxygen-density ρ_O.

We report in Fig. 1 a pictorial representation of the different GNR edges we have considered in this study, along with their characteristic periodicity L. In the left top line we show the clean zigzag and armchair GNRs.[23] The right top line (second line from top) represents the zigzag (armchair) oxygen-covered nanoribbons included in this work. Structures are chosen as to saturate each oxygen atom with two single bonds or a double one while other possible chemical bonding configurations are much less stable and are not included in the results. The edges are ordered with respect to increasing oxygen density and, at equal density, with respect to the energetics, from most favorable to least favorable. Nonaromatic edges[28,29] are indicated with a tilde (see Sec. V).

The density and zero-temperature edge-formation energy are reported in Table I. The free-energy G stability diagram is reported in Fig. 2. We note that three zigzag GNRs, named $\tilde{z}_{o2}$, z_{o4}, and z_{o5}, and three armchair GNRs, named a_{o11}, a_{o12}, and a_{o13}, have negative free energies, i.e., graphene should spontaneously break and form such ribbons if the experimental conditions allow to overcome the reaction barriers, as, for example, when nanoparticles, while sliding on graphene layers, are able to cut edges along their path.[9,10] We note that those experiments are performed in hydrogen atmosphere; in the case of oxygen atmosphere the reaction is more exothermic and could therefore be less controllable.

The thermodynamic stability diagram (Fig. 2) indicates that the armchair a_{o12} and the zigzag z_{o4} are the most stable configurations at low and high concentrations of atomic or molecular oxygen, respectively. However, the former one is more stable for nearly all negative values of the O_2 chemical

TABLE I. Formation energy $\mathcal{E}$ [defined as in Eqs. (1), (5), and (6)], oxygen density [$\rho_O = N_O/(2L)$] and nitrogen density [$\rho_N = N_N/(2L)$] for all the studied edges. The $\tilde{z}_{o2}$ edge, nonmagnetic within DFT–GGA calculations, is found to be magnetic when hybrid DFT functionals are used (Ref. 27). $^{\sim}$ Nonaromatic, * metallic edges, and † magnetic edges. We provide in Ref. 42 the equilibrium atomic structures of all the edges presently investigated.

	ρ_O (Å^{-1})	$\mathcal{E}_{O_2}$ (eV/Å)		ρ_O (Å^{-1})	$\mathcal{E}_{H_2O}$ (eV/Å)		ρ_N (Å^{-1})	$\mathcal{E}_{NH_3}$ (eV/Å)
$\tilde{z}_{57}^*$	0.000	0.9702	$\tilde{z}_{57}^*$	0.000	0.9702	$\tilde{z}_{57}^*$	0.000	0.9702
$\tilde{z}_0^\dagger$	0.000	1.1415	$\tilde{z}_0^\dagger$	0.000	1.1415	$\tilde{z}_0^\dagger$	0.000	1.1415
z_{o1}	0.270	0.3420	z_{oh1}	0.135	0.2086	z_{nh1}	0.135	0.1130
$\tilde{z}_{o2}^*$	0.405	−0.1991	z_{oh2}	0.135	0.2277	z_{nh2}	0.135	0.2291
$\tilde{z}_{o3}^*$	0.405	0.0570	z_{oh3}	0.135	0.7640	z_{nh3}	0.135	0.6512
z_{o4}	0.540	−0.5847	$\tilde{z}_{oh4}^\dagger$	0.202	0.2364	z_{nh4}	0.270	0.1527
z_{o5}	0.540	−0.5723	z_{oh5}	0.270	0.2042			
			z_{oh6}	0.270	0.2235			
			z_{oh7}	0.270	0.2518			
			z_{oh8}	0.270	0.2614			
			z_{oh9}	0.270	0.2619			
			$\tilde{z}_{oh10}^*$	0.405	1.4842			
a_0	0.000	0.9999	a_0	0.000	0.9999	a_0	0.000	0.9999
$\tilde{a}_{o1}^\dagger$	0.117	0.8258	a_{oh1}	0.117	0.4004	a_{nh1}	0.117	0.1643
a_{o2}	0.234	0.2915	a_{oh2}	0.234	0.2363	a_{nh2}	0.117	0.2808
a_{o3}	0.234	0.3204	a_{oh3}	0.234	0.2394	a_{nh3}	0.234	0.1605
a_{o4}	0.234	0.3776	a_{oh4}	0.234	0.2457	a_{nh4}	0.234	0.1880
$\tilde{a}_{o5}^\dagger$	0.234	0.4906	a_{oh5}	0.234	0.2466	a_{nh5}	0.234	0.3186
$\tilde{a}_{o6}^\dagger$	0.234	0.4940	a_{oh6}	0.234	0.2479	a_{nh6}	0.234	0.3310
$\tilde{a}_{o7}^\dagger$	0.234	0.5015	a_{oh7}	0.234	0.2715			
$\tilde{a}_{o8}^\dagger$	0.234	0.5744	a_{oh8}	0.234	0.3023			
a_{o9}	0.234	0.5868	a_{oh9}	0.234	0.3063			
a_{o10}	0.234	0.8212	a_{oh10}	0.234	0.3244			
a_{o11}	0.351	−0.0432						
a_{o12}	0.467	−0.5610						
a_{o13}	0.467	−0.2239						

potential, which suggests that the armchair edge should be the only thermodynamically stable one in ordinary experimental conditions going from ultravacuum to atmospheric concentration of molecular oxygen.

On the other hand, it is even more important to consider the presence of CO_2 molecules, either from the atmosphere or from the oxidation of edge carbon atoms. We can define, analogously to Eq. (1), an edge-formation energy per unit length with respect to carbon dioxide, which reads

$$\mathcal{E}_{CO_2} = \frac{1}{2L}\left(E^{ribb} - \left(N_C - \frac{N_O}{2}\right)E^{blk} - \frac{N_O}{2}E_{CO_2}\right). \quad (3)$$

By simple calculations one can easily show that

$$\mathcal{E}_{CO_2} = \mathcal{E}_{O_2} + \rho_O \Delta E_{CO_2}, \quad (4)$$

where ρ_O is, as above, the oxygen density per unit length and $\Delta E_{CO_2} = (E^{blk} + E_{O_2} - E_{CO_2})$ is the formation energy of molecular CO_2 from graphene and oxygen molecules, and

equals −3.76 eV in DFT-GGA. In other words, the chemical reaction $C^{blk} + O_2 \rightarrow CO_2$ is strongly exothermic, as well known from the fact that ordinary coal burns in oxygen once ignited. As a consequence, the molecular-oxygen thermodynamic stability scale equally holds for carbon dioxide, with a horizontal shift of ΔE_{CO_2}. Conversely, the molecular-oxygen thermodynamic stability scale must include a vertical line at $\mu_{O_2} = \Delta E_{CO_2} = -3.76$ eV: at higher oxygen densities no edge decoration can be thermodynamically more stable than CO_2. This, again, implies that only the armchair a_{o13} edge is realistically observable at thermodynamic equilibrium and oxygen concentration lower than the one which would induce spontaneous ignition of graphene with oxygen to produce CO_2.

IV. WATER AND AMMONIA

Besides oxygen, we considered GNR edges saturated with water or ammonia molecules. In these cases we restricted our
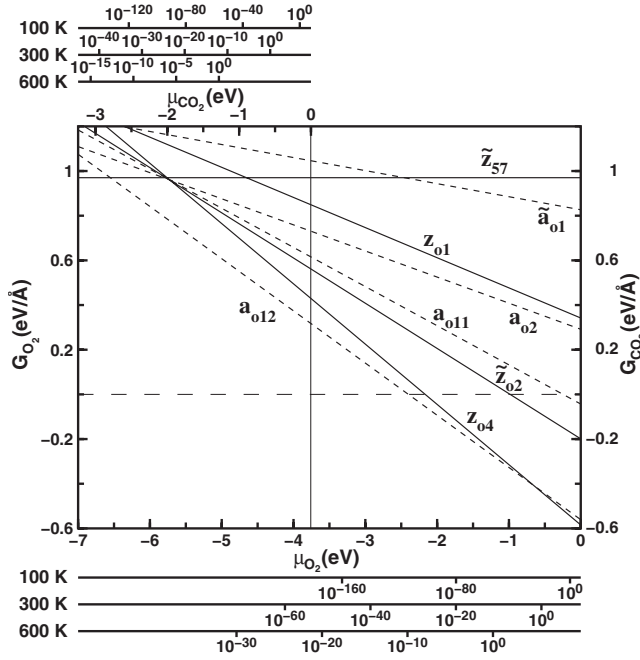
FIG. 2. Free energies versus chemical potential for the five most stable oxygen-terminated edges and of the clean one. The alternative bottom (top) axes show the pressure, in bar, of molecular O_2 (carbon dioxide) gas corresponding to the chemical potentials at T =100, 300, and 600 K.

study to O/H/N contents as fixed by the respective molecular stoichiometries, which corresponds to the description of experiments carried out in pure water or ammonia atmospheres. In principle, the full study of other stoichiometries would allow a more complete description of the thermodynamic properties as function of two independent chemical potentials, i.e., O and H (N and H) in the case of water (ammonia). However, the number of different possible edges is formidable, which would make these calculations extremely demanding, virtually impossible to carry out "by hand," and likely needing random-search optimizations.[41] Moreover, we only considered aromatic edge configurations,[28] with a few exceptions in the case of water. The zero-temperature edge-formation energies per length reads as follows:

$$\mathcal{E}_{H_2O} = \frac{1}{2L}(E^{ribb} - N_C E^{blk} - N_{H_2O} E_{H_2O}) \quad (5)$$

and

$$\mathcal{E}_{NH_3} = \frac{1}{2L}(E^{ribb} - N_C E^{blk} - N_{NH_3} E_{NH_3}) \quad (6)$$

in the case of water and ammonia, respectively. The restriction on aromatic edges implies that zigzag edges respect the 2-1-1 bond order rule for the dangling carbon bond that, as shown in Refs. 28 and 29, is the only aromatic configuration for zigzag GNRs. In the case of water, single dangling bonds are thus saturated by H atoms or OH groups while double bonds are saturated either by oxygen atoms or by H/OH-containing pairs (see Fig. 1, bottom row). In the case of ammonia, we considered all water-decorated structures, and replaced each O atom (OH group), by a NH (NH_2) group.
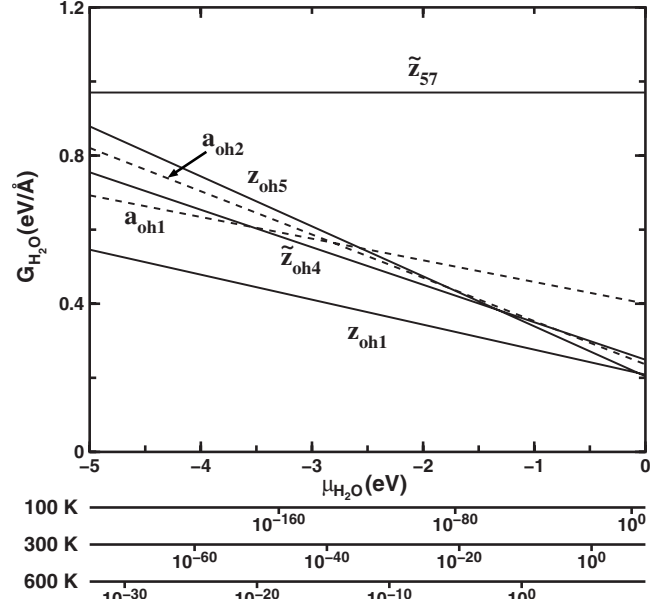

FIG. 3. Free energies versus chemical potential for the eight most stable edges after exposure to water, including the clean one. The bottom axes show the pressure, in bar, of molecular H_2O vapor corresponding to the chemical potentials at $T=100$, 300, and 600 K.

The formation energies are summarized in Table I, the corresponding thermodynamic stability plots are shown in Figs. 3 and 4. We provide in Ref. 42 the equilibrium atomic structures of all the edges presently investigated.

In the case of water, two main results are evident: the free energy is always positive, meaning that graphene would not spontaneously break to form edges in a water atmosphere. On the other hand, any freshly cut edge would be substantially stabilized in the presence of water by the saturation of
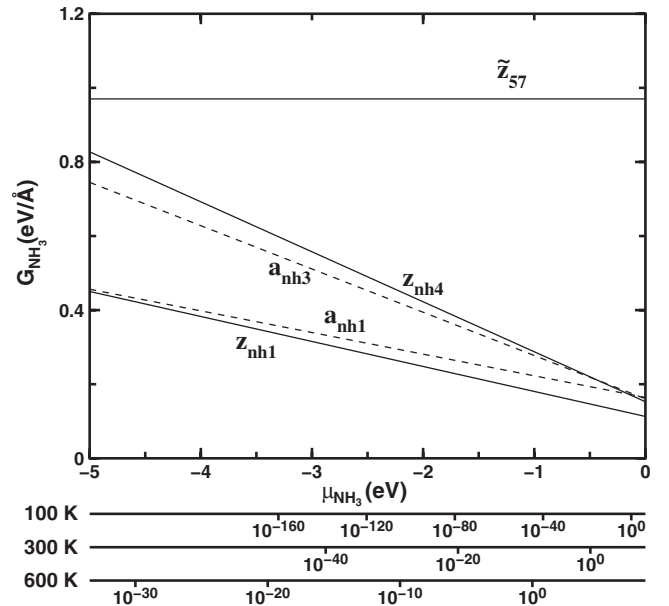

FIG. 4. Free energies versus chemical potential for the four most stable edges after exposure to ammonia and of the clean one. The bottom axes show the pressure, in bar, of molecular NH_3 vapor corresponding to the chemical potentials at $T=100$, 300, and 600 K.
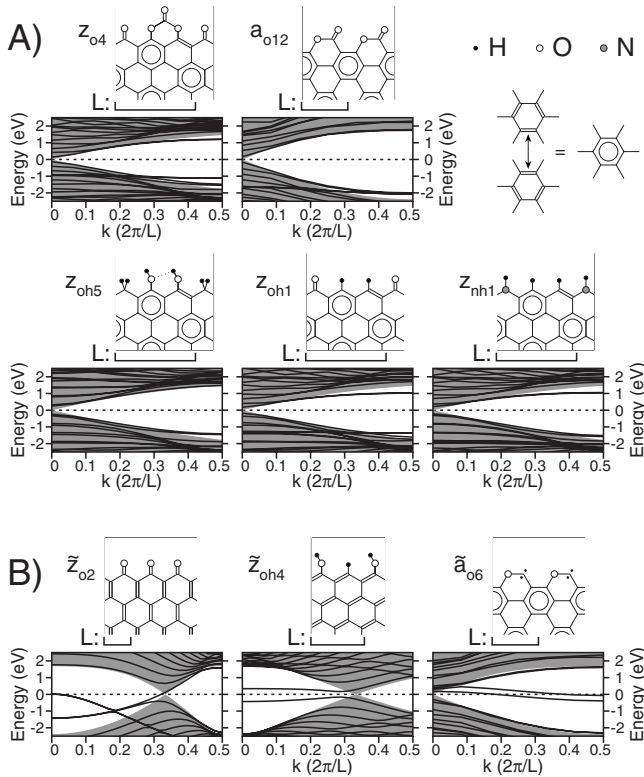
FIG. 5. (A) Scheme and electronic band structure of the five most stable oxygen-, water- and ammonia-terminated edges of a graphene nanoribbon. Carbon-carbon bonds are represented with the standard notation while hydrogen, oxygen, and nitrogen atoms are the small circles. The structures are periodic along the ribbon edge with periodicity L. The gray area corresponds to the electronic bands allowed in bulk graphene. The dashed line is the Fermi level. The top-right inset displays the standard representation of the aromatic carbon ring. (B) Three examples of "metallic/magnetic" edges (see the definition in the text). $\tilde{z}_{o2}$, nonmagnetic within DFT–GGA calculations, is found to be magnetic when hybrid DFT functionals are used (Ref. 27); $\tilde{z}_{oh4}$ and $\tilde{a}_{o6}$ both magnetic. The $\tilde{a}_{o6}$ structure is nonaromatic according to our definition, since the two small dots represent a diradical, which is the only representation compatible with the carbon chemical valence.

its dangling bonds with O/H/OH groups. The other result is that z_{oh1} is the most stable configuration at any chemical potential. This means that, in principle, the presence of oxygen favors the armchair edges while the presence of water favors the zigzag ones. In the case of ammonia, free energies are always positive, and the z_{nh1} zigzag GNR is the most stable one, in correspondence to z_{oh1} in presence of water.

V. DISCUSSION

We have shown in our previous works on hydrogen-decorated edges[28] and GNRs (Ref. 29) that a number of different edge structures with different electronic/magnetic properties compete for thermodynamic stability at different hydrogen concentrations, and that they should be considered in order to provide results of practical use to experimentalists. In particular, we showed that an important hint on the structural and chemical stability of GNR edges comes from the well-known organic chemistry structural properties of polycyclic aromatic hydrocarbons (PAHs), large molecules consisting of fused carbon rings. According to the so-called Clar's rule,[43,44] the most stable structures for PAHs are the ones maximizing the number of Clar sextets.

In bulk graphene all π electrons take part in the formation of Clar sextets. In this arrangement, one out of three hexagons is a Clar sextet. We define, as in Refs. 28 and 29, aromatic edges as those allowing for the same 1/3 density of benzenoid rings as bulk graphene and in which every carbon atom is fully saturated (it has four covalent bonds). Conversely, in nonaromatic edges the 1/3 bulk-graphene density of benzenoid rings is incompatible with a full saturation of all carbon dangling bonds. These edges are indicated with a $\sim$ in their label. This density can only be recovered at the price of having carbon atoms with more or less than four covalent bonds. In the presence of magnetism such over/underbonding can be interpreted as radicals, as in the edge labeled $\tilde{a}_{o6}$ (see Fig. 5, panel B, and discussion in Ref. 29).

As shown in Fig. 1 and in Table I, we find that, except for $\tilde{z}_{o2}$ and analogously to the case of hydrogen-saturated edges, the energetically most stable ones are aromatic. In the case of water, the $\tilde{z}_{oh4}$ edge is the only relatively stable nonaromatic configuration. In Fig. 5 we report the electronic band structure, close to the Fermi level, of the most stable and interesting edges. The gray-shaded areas indicate the edge-projected bulk bands. The full lines correspond to GNR electronic states. Bands outside the gray-shaded area are electronic states exponentially localized at the edges (edge states).

In line with the results of Ref. 28, in Table I and in Fig. 5 we show that nonaromatic edges invariably display edge states at the Fermi level that can split up and thus induce a magnetic character of the edge. In absence of such splitting those states are only partially occupied, giving rise to metallic behavior. On the contrary, aromatic edges either do not possess edge states (as shown in Fig. 5, panel A) or such states are fully empty or occupied [as a_0 (Ref. 28)].

VI. CONCLUSIONS

In conclusion, our *ab initio* DFT calculations indicate that neutral graphene edges, in the presence of molecular species typical of experimental conditions, are stabilized by decoration with double-bonding O/NH groups or single-bonding OH/H/NH$_2$ groups. In contrast to the case of hydrogen saturation, for each molecular species we observe only very few possible edges in the thermodynamical stability diagram, namely, an armchair edge in the case of oxygen and one zigzag edge in the case of water and in the case of ammonia. This observation might help experimentalists in discriminating between zigzag and armchair edges and their mixtures according to the chemical composition of the atmosphere in which GNRs are obtained.

[1] K. Nakada, M. Fujita, G. Dresselhaus, and M. S. Dresselhaus, Phys. Rev. B **54**, 17954 (1996).

[2] K. S. Novoselov, A. K. Geim, S. V. Morozov, D. Jiang, Y. Zhang, S. V. Dubonos, I. V. Grigorieva, and A. A. Firsov, Science **306**, 666 (2004).

[3] M. Y. Han, B. Ozyilmaz, Y. Zhang, and P. Kim, Phys. Rev. Lett. **98**, 206805 (2007).

[4] Z. H. Chen, Y.-M. Lin, M. J. Rooks, and P. Avouris, Physica E **40**, 228 (2007).

[5] L. Tapasztó, G. Dobrik, P. Lambin, and L. P. Biró, Nat. Nanotechnol. **3**, 397 (2008).

[6] P. Nemes-Incze, G. Magda, K. Kamarás, and L. Péter Biró, Nano Res. **3**, 110 (2010).

[7] X. Li, X. Wang, L. Zhang, S. Lee, and H. Dai, Science **319**, 1229 (2008).

[8] X. Wang, Y. Ouyang, X. Li, H. Wang, J. Guo, and H. Dai, Phys. Rev. Lett. **100**, 206803 (2008).

[9] S. S. Datta, D. R. Strachan, S. M. Khamis, and A. T. Charlie Johnson, Nano Lett. **8**, 1912 (2008).

[10] L. Ci, Z. Xu, L. Wang, W. Gao, F. Ding, K. F. Kelly, B. I. Yakobson, and P. M. Ajayan, Nano Res. **1**, 116 (2008).

[11] D. V. Kosynkin, A. L. Higginbotham, A. Sinitskii, J. R. Lomeda, A. Dimiev, B. Katherine Price, and J. M. Tour, Nature (London) **458**, 872 (2009).

[12] L. Jiao, L. Zhang, X. Wang, G. Diankov, and H. Dai, Nature (London) **458**, 877 (2009).

[13] L. Jiao X. Wang, G. Diankov, H. Wang, and H. Dai, Nat. Nanotechnol. **5**, 321 (2010).

[14] L. C. Campos, V. R. Manfrinato, J. D. Sanchez-Yamagishi, J. Kong, and P. Jarillo-Herrero, Nano Lett. **9**, 2600 (2009).

[15] C. O. Girit, J. C. Meyer, R. Erni, M. D. Rossell, C. Kisielowski, L. Yang, C.-H. Park, M. F. Crommie, M. L. Cohen, S. G. Louie, and A. Zettl, Science **323**, 1705 (2009).

[16] X. T. Jia, M. Hofmann, V. Meunier, B. G. Sumpter, J. Campos-Delgado, J. M. Romo-Herrera, H. Son, Y.-P. Hsieh, A. Reina, J. Kong, M. Terrones, and M. S. Dresselhaus, Science **323**, 1701 (2009).

[17] A. Yamashiro, Y. Shimoi, K. Harigaya, and K. Wakabayashi, Phys. Rev. B **68**, 193410 (2003).

[18] L. Pisani, J. A. Chan, B. Montanari, and N. M. Harrison, Phys. Rev. B **75**, 064418 (2007).

[19] Y. W. Son, M. L. Cohen, and S. G. Louie, Nature (London) **444**, 347 (2006).

[20] E. J. Kan, Z. Li, J. Yang, and J. G. Hou, Appl. Phys. Lett. **91**, 243116 (2007).

[21] O. V. Yazyev and M. I. Katsnelson, Phys. Rev. Lett. **100**, 047209 (2008).

[22] S. Okada, Phys. Rev. B **77**, 041408 (2008).

[23] P. Koskinen, S. Malola, and H. Häkkinen, Phys. Rev. Lett. **101**, 115502 (2008).

[24] B. Huang, F. Liu, J. Wu, B. L. Gu, and W. Duan, Phys. Rev. B **77**, 153411 (2008).

[25] F. Cervantes-Sodi, G. Csányi, S. Piscanec, and A. C. Ferrari, Phys. Rev. B **77**, 165427 (2008).

[26] O. Hod, V. Barone, J. E. Peralta, and G. E. Scuseria, Nano Lett. **7**, 2295 (2007).

[27] A. Ramasubramaniam, Phys. Rev. B **81**, 245413 (2010).

[28] T. Wassmann, A. P. Seitsonen, A. M. Saitta, M. Lazzeri, and F. Mauri, Phys. Rev. Lett. **101**, 096402 (2008).

[29] T. Wassmann, A. P. Seitsonen, A. M. Saitta, M. Lazzeri, and F. Mauri, J. Am. Chem. Soc. **132**, 3440 (2010).

[30] G. Lee and K. Cho, Phys. Rev. B **79**, 165440 (2009).

[31] J. Berashevich and T. Chakraborty, Phys. Rev. B **81**, 205431 (2010).

[32] M. Wu, X. Wu, Y. Gao, and X. C. Zeng, Appl. Phys. Lett. **94**, 223111 (2009).

[33] M. Wu, X. Wu, and X. C. Zeng, J. Phys. Chem. C **114**, 3937 (2010).

[34] X. H. Zheng, X. L. Wang, T. A. Abtew, and Z. Zeng, J. Phys. Chem. C **114**, 4190 (2010).

[35] S. S. Yu, W. T. Zheng, and Q. Jiang, IEEE Trans. Nanotechnol. **9**, 243 (2010).

[36] P. Giannozzi *et al.*, J. Phys.: Condens. Matter **21**, 395502 (2009); http://www.quantum-espresso.org/

[37] J. P. Perdew, K. Burke, and M. Ernzerhof, Phys. Rev. Lett. **77**, 3865 (1996).

[38] G. X. Qian, R. M. Martin, and D. J. Chadi, Phys. Rev. B **38**, 7649 (1988).

[39] C. L. Bailey, A. Wander, S. Mukhopadhyay, B. G. Searle, and N. M. Harrison, Science and Technology Facilities Council, Daresbury Laboratory Technical Report 2007–004, 2007 (unpublished).

[40] M. W. Chase, Jr., C. A. Davies, J. R. Downey, Jr., D. J. Frurip, R. A. McDonald, and A. N. Syverud, *JANAF Thermochemical Tables*, Journal of Physical and Chemical Reference Data Vol. 14, Suppl. 1, 3rd ed. (American Chemical Society and American Institute of Physics, 1985).

[41] C. J. Pickard and R. J. Needs, Phys. Rev. Lett. **97**, 045504 (2006).

[42] See supplementary material at http://link.aps.org/supplemental/10.1103/PhysRevB.82.115425 for the equilibrium atomic structures of all the edges presently investigated.

[43] E. Clar, *Polycyclic Hydrogarbons* (Academic Press, London, 1964).

[44] E. Clar, *The Aromatic Sextet* (Wiley, New York, 1972).